Fundamental Frequency and Regularity of Cardiac Electrograms With Fourier Organization Analysis

Óscar Barquero-Pérez, José Luis Rojo-Álvarez*, *Member, IEEE*, Antonio J. Caamaño, Rebeca Goya-Esteban, Estrella Everss, Felipe Alonso-Atienza, Juan José Sánchez-Muñoz, and Arcadi García-Alberola

***Abstract*—Dominant frequency analysis (DFA) and organization analysis (OA) of cardiac electrograms (EGMs) aims to establish clinical targets for cardiac arrhythmia ablation. However, these previous spectral descriptions of the EGM have often discarded relevant information in the spectrum, such as the harmonic structure or the spectral envelope. We propose a fully automated algorithm for estimating the spectral features in EGM recordings This approach, called Fourier OA (FOA), accounts jointly for the organization and periodicity in the EGM, in terms of the fundamental frequency instead of dominant frequency. In order to compare the performance of FOA and DFA–OA approaches, we analyzed simulated EGM, obtained in a computer model, as well as two databases of implantable defibrillator-stored EGM. FOA parameters improved the organization measurements with respect to OA, and averaged cycle length and regularity indexes were more accurate when related to the fundamental (instead of dominant) frequency, as estimated by the algorithm ($p < 0.05$ comparing f_0 estimated by DFA and by FOA). FOA yields a more detailed and robust spectral description of EGM compared to DFA and OA parameters.**

***Index Terms*—Dominant frequency, electrogram, Fourier series, organization, spectrum, ventricular fibrillation (VF).**

I. Introduction

ANALYSIS of intracardiac electrograms (EGMs) in cardiac electrophysiology has often been addressed by using time-domain parameters, such as activation times and voltage amplitudes [1], [2]. Though, early descriptions of EGM in the frequency domain had few implications for clinical practice [3], [4]. However, there has been a recent increase in interest in its application to the clinical environment, and several clinical targets for atrial fibrillation (AF) ablation use the EGM spectral representation. These targets aim to give a regular description in the frequency domain, in terms of low cycle length (CL) and/or high regularity regions [5], [6]. Such spectral features have been used both in electrical and in optical mapping recordings, during AF and ventricular fibrillation (VF) [7]–[11]. In [12], EGM from implantable cardioverter defibrillators (ICDs) were also analyzed during sinus rhythm (SR) and ventricular tachycardia (VT).

Two complementary approaches have been mainly followed in spectral analysis applied to cardiac mapping systems: fominant frequency analysis (DFA) and organization analysis (OA) [7], [13]. The former aims to characterize the EGM periodicity using the averaged CL of a nonpurely periodic rhythm (usually AF or VF), whereas the latter quantifies the signal energy that remains unexplained by that periodicity. However, these descriptions have often discarded relevant information of the spectrum, such as the harmonic structure or the spectral envelope. Moreover, it is not always guaranteed that a dominant frequency will give a good estimation of the averaged CL. Singh *et al.* [14] showed that there is a poor correlation between the EGM average CL and the dominant frequency in patients with persistent AF. These drawbacks can lead to incomplete understanding of the information in DFA and OA spectral parameters, and they are further explored in this paper.

This paper proposes a unified, simple, and automatic processing algorithm for: 1) improving the parameters estimated from DFA and OA and 2) giving more detailed information about the spectral EGM structure. The proposed method, called Fourier OA (FOA), uses a least squares (LS) approximation of the EGM using a modified harmonic Fourier-series signal model, closely related to the OA description, accounting for narrow-band fluctuations of each component in the Fourier series. The fundamental frequency, used in our method as an estimation of the inverse of the CL, is first estimated, according to the best LS fit to the EGM as a function of the signal model in terms of this parameter. Then, a set of parameters from the best model is used to describe the spectral structure and organization of the signal.

The scheme of the paper is as follows. Section II summarizes the parameters from DFA and OA for EGM spectral characterization. In Section III, the FOA algorithm is proposed. We analyze the performance of FOA compared to DFA and OA using computer simulations (see Section IV) and using two databases of clinical signals of ICD-stored EGM recordings (see Section V). Section VI contains the discussion of this paper. A preliminary version of this paper has been presented in [15].

II. Background on DFA and OA

Spectral parameters for DFA and OA have been defined under the implicit assumption that the underlying signal consists of an almost-periodic component plus an irregular

Manuscript received November 5, 2009; revised February 2, 2010 and April 13, 2010; accepted April 16, 2010. Date of publication May 10, 2010; date of current version August 18, 2010. This work was supported in part by the Spanish Government under Project URJC-CM-2008-CET-3732, Project TEC2007-68096-C02-01/TCM, and Project TEC2009-12098. *Asterisk indicates corresponding author.*

Ó. Barquero-Pérez, A. J. Caamaño, R. Goya-Esteban, E. Everss, and F. Alonso-Atienza are with the Department of Signal Theory and Communications, University Rey Juan Carlos, Fuenlabrada, Madrid 28943, Spain.

*J. L. Rojo-Álvarez is with the Department of Signal Theory and Communications, University Rey Juan Carlos, Fuenlabrada, Madrid 28943, Spain (e-mail: joseluis.rojo@urjc.es).

J. J. Sánchez-Muñoz and A. García-Alberola are with the Arrhythmia Unit, Hospital Virgen de la Arrixaca, Murcia 30120, Spain.

Color versions of one or more of the figures in this paper are available online at http://ieeexplore.ieee.org.

Digital Object Identifier 10.1109/TBME.2010.2049574

component [7], [13]. On the one hand, DFA aims to determine the averaged CL of the almost-periodic component in an EGM, and for this purpose, dominant frequency f_d has been defined as the frequency of the maximal absolute value of its spectrum $P(f)$. The parameter f_d is obtained either directly from the EGM spectrum, or by using an auxiliary signal, obtained by filtering and rectifying the EGM [16]. This last method is commonly used as an automatic procedure for obtaining the averaged CL estimation of an EGM. An additional parameter, called dominant frequency bandwidth $bw(f_d)$, is sometimes obtained. This parameter is defined as the difference between the upper and lower frequencies for which the spectral maximum peak falls to 75% of its value.

OA takes a different approach and aims to measure the relative contribution of the almost-periodic component of an EGM in terms of its signal power. Conventional organization parameters are defined in the frequency domain. The first step of the calculation is to estimate the underlying CL (usually from DFA). Next, the power of the components in a predetermined narrowband around either the fundamental peak or the harmonic peaks is used to account for the relevance of the almost-periodic component. Typically, two parameters are used. The regularity index ri, which was originally defined as the ratio of power in the dominant frequency bandwidth and the total power in the band of interest. In this paper, we use the the B band (2–30 Hz for AF and 2–15 Hz in VF) [5], [17]. Later, the organization index oi was defined. This is the ratio of the power in the fundamental frequency bandwidth, combining up to four harmonic peaks, and the total power in the B band [13], [18].

Though highly informative, the parameters yielded by DFA and OA (f_d, $bw(f_d)$, oi, and ri) give an incomplete spectral description of the signals. Another important descriptor is the spectral envelope, which for a purely periodic signal is given by the Fourier transform of a single cycle. For an almost-periodic signal, the spectral envelope is still (roughly) related to the averaged Fourier transforms of consecutive cycles. For EGM analysis purposes, the spectral envelope can be seen as the spectrum of an isolated arrhythmia complex, which is dependent on the morphology of the EGM, but independent from its CL.

In a purely periodic signal, harmonic frequencies are the integer multiples of fundamental frequency f_0, i.e., $f_k = kf_0$. DFA and OA parameters have been used to analyze the differences between spontaneous and induced VF episodes [19], and to study the self-termination of VF episodes [20] in ICD-stored EGM. The spectral envelope yields a spectral representation that has no harmonic structure, and hence, it contains explicit information about the underlying physiological phenomena, as well as about the acquisition characteristics. In some works, the spectral profile of the harmonics showed significant differences between patients with inferior and anterior myocardial infarction, whereas the differences in f_d, f_0 from DFA, and oi were nonsignificant [21]. There are other works where the spectral envelope is used as a feature in a discrimination scheme of ventricular arrhythmias [22], [23].

Parameters from DFA and OA can even become inaccurate in some conditions, given that f_d will not always be the same as f_0. This risk holds, even when using the automatic algorithm in [16]. An operating definition for f_0 in the presence of harmonic structure was presented in [19]–[21]. It is defined as the averaged interharmonic separation. According to the theoretical properties of the Fourier transform of periodic signals, this yields an estimation of the inverse of the CL, when harmonic structure is present in the EGM [24]. This definition of fundamental frequency, however, has not yet been implemented in an automatic signal-processing algorithm.

III. Fourier Organization Analysis

In this section, we propose the FOA algorithm, as a generalized version of both DFA and OA, by using the well-known principles of spectral analysis and signal approximation. First, we present the signal model and the approximation using LS principles. Then, we describe the proposed strategy for automatic estimation of f_0. Finally, periodicity and organization of EGM parameters used within the FOA algorithm are described.

A. FOA Signal Model

Let EGM(t) be a continuous-time EGM signal. If it was a purely periodic signal with fundamental period T_0, its Fourier series representation would be given by $\text{EGM}(t) = \sum_{k=1}^{K} A_k \cos\left(2\pi\left(kf_0\right)t + \phi_k\right)$, where $f_0 = 1/T_0$ is the fundamental frequency. A_k and ϕ_k represent the amplitude and phase for each harmonic component, respectively. K represents the number of harmonics.

Three additional elements can be introduced into this signal model. First, additive noise can be present, denoted by $e(t)$. Second, we work with a digitized version of EGM(t) during a given acquisition time interval, which yields N samples acquired at a rate of f_s samples per second. Under these conditions, the spectral resolution of a nonparametric Fourier-based spectral analysis procedure is about $\Delta = f_s/N$ Hz. Third, EGM(t) will not be purely periodic in real recordings, but it will be almost- or near-periodic. This can be observed by the presence of narrowband structure (harmonic peaks) in the signal spectrum.

In the case of OA parameters, spectral components in a narrow bandwidth of the spectral peaks contribute to the quantification of the signal regularity, e.g., ri, as defined in [5]. It is computed by taking into account the power at the dominant frequency and at its adjacent frequencies. In a Fourier-based spectral analysis, this correspond to the spectral resolution Δ. A similar idea can be included in our model by considering two additional sinusoidal components for each harmonic peak, whose frequencies are the harmonic component plus and minus Δ Hz. The signal model for EGM(t) is given by

$$\begin{aligned}\text{EGM}(t) = &\sum_{k=1}^{K} A_k \cos\left(2\pi(kf_0)t + \phi_k\right) \\ &+ \sum_{k=1}^{K} A_k^- \cos\left(2\pi(kf_0 - \Delta)t + \phi_k^-\right) \\ &+ \sum_{k=1}^{K} A_k^+ \cos\left(2\pi(kf_0 + \Delta)t + \phi_k^+\right) + e(t)\end{aligned} \tag{1}$$

where A_k^+, A_k^-, ϕ_k^+, and ϕ_k^- are the amplitudes and phases related to the near-periodicity associated with the harmonics. This signal model can be expressed in an abbreviated form $\text{EGM}(t) = s_{f_0}(t) + e(t)$, where $s_{f_0}(t)$ denotes the organized or near-periodic component of $\text{EGM}(t)$ that is associated with f_0. Recall that f_0 corresponds to the inverse of the averaged CL, or fundamental period T_0, in the time domain. The model parameters $\{A_k, A_k^+, A_k^-, \phi_k, \phi_k^+, \phi_k^-\}$ can be estimated by using the discrete-time version of the EGM, (1), i.e, $\text{EGM}[n] = \text{EGM}(n/f_s)$, where $n \in \mathbb{Z}$ is a discrete-time integer index, by using an LS projection onto a Hilbert signal space of sampled sinusoids containing the fluctuations. Therefore, we are simply proposing a Fourier series expansion that considers two additional sinusoidal neighbor components for each harmonic component, the coefficients for this expansion being estimated using LS.

In order to use the FOA signal model in (1), the following steps are necessary.

1) *Estimation of f_0 and periodicity description*. This step provides the estimation of the main rhythm. We propose an automatic method that searches for the argument that minimizes the mean square error (MSE) for FOA signal model in (1) as a function of f_0.
2) *Signal model fitting and organization description*. In this step, FOA signal model is fitted to the EGM, using f_0^*, as estimated in the previous step. The coefficients of the signal model are again computed by LS procedure. Therefore, coefficients are estimated by minimizing, $\|S\mathbf{a} - \text{EGM}\|_2$, where $\mathbf{a}$ are the coefficients of the model, $\mathbf{a} = \{A_k, A_k^+, A_k^-; k = 1, \ldots, K\}$, S is the matrix of sine and cosine base signals, and EGM is the column-vector EGM. Coefficients are estimated by using the Moore–Penrose pseudoinverse, $\mathbf{a} = (S^T S)^{-1} S^T \text{EGM}$.

These steps are further explained in the following sections.

B. Automatic Estimation of f_0

We have previously introduced the FOA signal model assuming that f_0 is known, but in practice, f_0 is also an unknown parameter and it has to be estimated. We propose a simple automatic estimation method using the FOA signal model, consisting of fitting the signal model in (1). Fitting means we need to calculate coefficients using LS, for a set of values of f_0 in an adequate frequency range for search, $f_0 \in [f_l, f_h]$ Hz. Let us denote the signal model fitted for each f_0 in that range, by $\hat{s}_{f_0}(t)$. The MSE between the signal and the fitted model is computed as a function of f_0, i.e., $\text{MSE}(f_0) = \| \text{EGM}[n] - \hat{s}_{f_0}[n]\|^2$. The best value of f_0 is then the argument that minimizes $\text{MSE}(f_0)$, i.e.,

$$f_0^* = \arg\min_{f_0} \text{MSE}(f_0), \quad f_0 \in [f_l, f_h] \text{ Hz}. \tag{2}$$

where f_0^* is the optimum value to be used as the fundamental frequency for the FOA signal model (see Fig. 2).

In some cases, subharmonics of f_0 have been observed to give low MSE values, yielding inadequate f_0^* estimations. These cases can be readily identified and corrected by noting that the spectral profile becomes a strongly oscillating series.

C. FOA Parameters

The implicit relationship between the signal model in (1) and parameters oi and ri allows us to define an index for quantifying the regularity of the signal. This is given by the power ratio between the near-periodic component and the EGM. For the estimated fundamental frequency f_0^*, the model is fitted to the signal using LS procedure, and then, the EGM can be modeled as follows:

$$\text{EGM}[n] = \hat{s}_{f_0^*}[n] + e[n]. \tag{3}$$

We can simply take energy ratios, and then, regularity coefficients are calculated as follows:

$$p_1 = \frac{\|\hat{s}_{f_0^*}[n]\|^2}{\|\text{EGM}[n]\|^2}, \quad p_e = \frac{\|e[n]\|^2}{\|\text{EGM}[n]\|^2}. \tag{4}$$

Note that p_1 is just a generalization of oi and ri parameters. Also note that p_e accounts not only for the noise, but also for any additional component not included in p_1 and not related to f_0^*. Previous parameters quantifying organization (oi and ri) implicitly assume a defined periodicity in the signal; hence, organization being referred to the quantification of the agreement with that periodicity. We followed a similar framework for parameter p_1 measuring the agreement of the signal with periodicity in f_0. This represents an operative definition for the organization concept, in which periodicity and organization are jointly searched, and the chosen periodicity is given by the higher organization that can be obtained from the adjustment of the near-harmonic signal model.

Other spectral parameters can be readily obtained from signal model (1). Trivially, dominant frequency is simply the frequency for which the maximum spectral amplitude occurs, i.e., $f_d = \arg\max_f \{A_k^-, A_k, A_k^+; k = 1, \ldots, K\}$. We can also define the set of modulus parameters as $M_k = A_k^- + A_k + A_k^+$, which represents the modulus for the kth component, taking into account the kth harmonic and its corresponding sinusoidal fluctuation components.

A good estimation of f_0^* is a fundamental step in the spectral analysis of EGM signal recordings, since not only does this parameter accounts for the CL, but also all the other organization parameters are directly related to it. This also holds for DFA and OA parameters. As previously stated, the use of f_d instead of f_0^* can be misleading in EGM with non-low-pass spectral envelopes, and even the use of the automated algorithm in [25] can give incorrect estimates if it is not subsequently supervised. In particular, when applying FOA, slight deviations from an adequate value of f_0^* will reduce the value of the p_1 coefficient, leading to inaccurate interpretations of the EGM organization and irregularity. The number of harmonics (K) to be used in the model is also a practical issue, and it has to be previously fixed. In this paper, our simple approach consisted of estimating it by dividing the signal bandwidth to the value of f_0^*.

In summary, FOA is closely related to conventional nonparametric spectral analysis and to DFA and OA. Its main advantage is that FOA gives a unified and detailed description of the spectrum and organization by the application of an automatic algorithm.

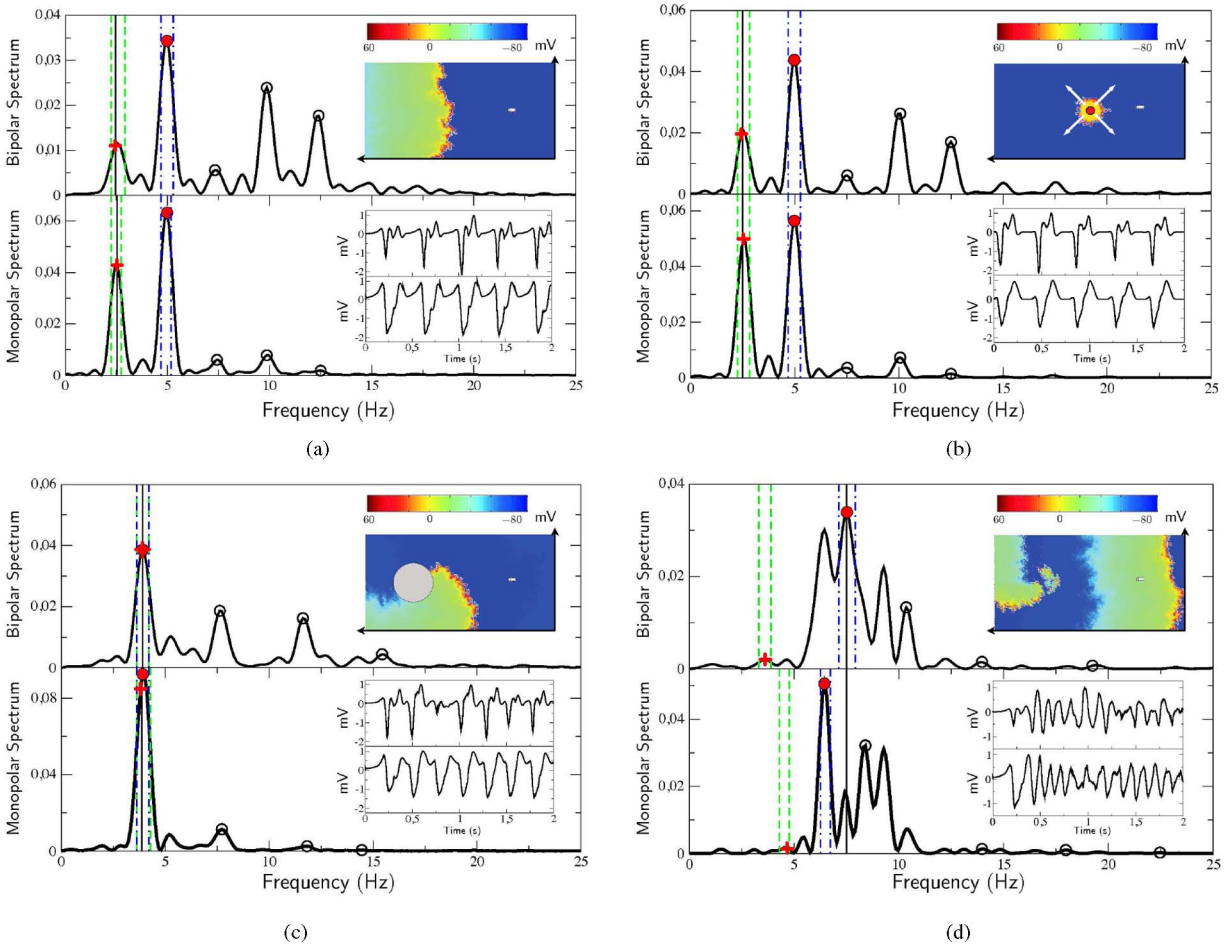

Fig. 1. Simulation results. EGM and spectra for bipolar and monopolar recordings in each simulated electrophysiological condition. (a) Plane wavefront. (b) Focal activation. (c) Anchored rotor. (d) Fibrillatory conduction. Spectral peaks are denoted by crosses (f_0), solid circle (f_d), and third to fifth harmonics (empty circles) estimated by DFA–OA method. Dotted vertical lines in the spectra indicate $bw(f_0)$ and $bw(f_d)$. Solid vertical lines in the spectra indicate f_0 estimated by FOA method. Inbox subpanels show a snapshot of the (top) action potential simulation and (bottom) simulated EGM.

IV. Simulations

A. Computer Model

A computer model [26] was used to simulate examples of monopolar and bipolar EGM recorded in different and simple electrophysiological conditions (see Fig. 1). In brief, a rectangular grid of 1×2 cm (80 cell groups per centimeter) was constructed for discretizing a 2-D tissue model. Excitation dynamics were given by a cellular automaton with three states (rest, activated, and refractory), where transitions were controlled by static restitution curves of the action potential duration and of conduction velocity in terms of the diastolic interval. Voltage levels were calculated by using a prototype action potential, whose time duration was modified according to restitution properties. Diffusion rules yielded action potential propagation along the tissue. An EGM recording model, according to the volume conductor equation in a homogeneous medium [27], was tuned for modeling simultaneous monopolar and bipolar recordings. A monopolar electrode was placed at $x = 1.5$ cm, $y = 0.5$ cm, and 0.2 cm height. The bipolar electrode configuration consisted of that electrode at the positive pole, and a negative electrode at $x = 1.52$ cm, $y = 0.52$ cm, and 0.2 cm height. Simulated EGM were recorded at 1600 samples per second (see [26] for details).

Several electrophysiological conditions were simulated: 1) sustained line stimulation from the left border (pacing rate of 400 ms), yielding a plane wavefront; 2) point stimulation (pacing rate of 400 ms) from a focal point at $x = 1$ cm and $y = 0.5$ cm; 3) anchored rotor around a circular obstacle (0.4 cm diameter infracted region); and 4) fibrillatory activity. The two last conditions were generated by using a standard $S1 - S2$ stimulation protocol, and the simple tissue and acquisition model contained all the necessary information for an easy comparison between the tissue activity and the recorded EGM in these example conditions [26]. Each simulation was run for 2 s, as this was long enough duration to include several cycles of tachycardia and fibrillation in all cases.

B. Analysis Methods

The FOA algorithm applied to the simulated EGM signals consisted of the steps described previously in Section III. Specifically, f_0^* was first estimated, the signal model in (1) was then fitted using LS, and organization (p_1 and p_e) and spectral envelope ($M_k, f_d, A_k, A_k^+, A_k^-$) parameters were obtained. Fig. 2

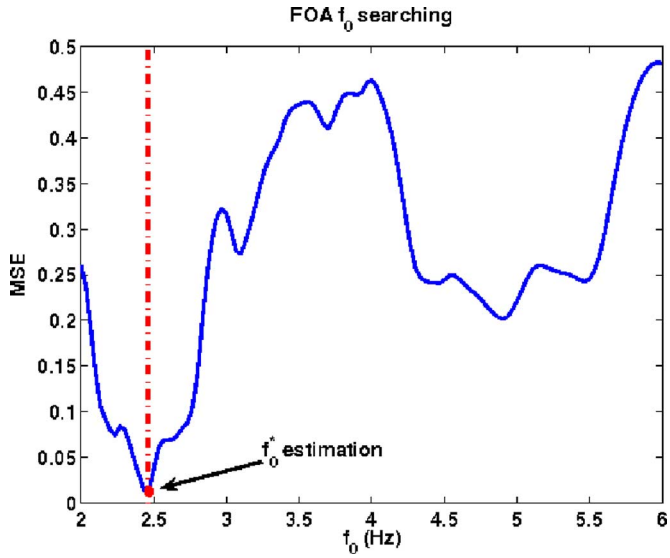

Fig. 2. Example of MSE for estimating f_0^* in plane-wavefront EGM simulation with FOA procedure. Note that the better the f_0 estimation, the lower the MSE.

TABLE I
RESULTS OF DFA, OA, AND FOA IN SIMULATED EGM

		Plane		Focal		Anchored		Fibrillatory	
		M	B	M	B	M	B	M	B
MFR (Hz)		2.48		2.50		3.88		7.12 / 7.08*	
Time	$CL\ (ms)$	400	400	400	400	250	250	143	125
	$CL^{-1}\ (Hz)$	2.5	2.5	2.5	2.5	4.0	4.0	6.9	8
DFA and OA	$f_0\ (Hz)$	2.54	2.44	2.54	2.44	3.81	3.91	4.69	3.61
	$f_d\ (Hz)$	4.98	4.98	4.98	4.88	3.91	3.91	6.45	7.52
	$P_n(f_d)$	63	34	56	43	93	39	50	34
	$P_n(f_0)$	43	11	50	20	85	39	2	2
	$P_n(f_2)$	63	34	56	44	11	19	32	34
	$P_n(f_3)$	6	6	4	6	2	3	14	13
	$P_n(f_4)$	8	24	7	26	0.5	11	1	1
	$P_n(f_5)$	2	18	1	17	0.3	.3	0.3	0.7
	$bw(f_0)\ (Hz)$	0.49	0.68	0.59	0.59	0.68	0.59	0.49	0.59
	$bw(f_d)\ (Hz)$	0.49	0.58	0.59	0.59	0.59	0.59	0.49	0.78
	oi	0.99	0.80	0.99	0.92	0.83	0.66	0.53	0.47
	ri	0.45	0.26	0.41	0.30	0.69	0.31	0.32	0.30
FOA	$f_0\ (Hz)$	2.47	2.43	2.50	2.50	3.87	3.90	7.49	7.53
	M_0	0.63	0.30	0.55	0.39	0.99	0.50	0.76	0.67
	M_2	0.87	0.44	0.53	0.49	0.50	0.47	0.10	0.12
	M_3	0.29	0.21	0.17	0.18	0.31	0.50	0.04	0.05
	M_4	0.38	0.45	0.20	0.38	0.15	0.28	0.03	0.02
	M_5	0.23	0.44	0.10	0.30	0.11	0.17	0.01	0.01
	p_1	0.98	0.90	0.96	0.96	0.89	0.77	0.59	0.52
	p_e	0.02	0.10	0.04	0.04	0.11	0.23	0.41	0.48

Parameters from $P_n(f)$ are reported as its value $\times 10^3$. *The second value was computed averaging action potentials from a square of nine cells right below the recording electrode.

shows an example of MSE as a function of f_0 in FOA procedure, for the case of the plane wavefront.

For conventional parameters, the automatic procedure in DFA was used to calculate f_0 in a filtered and rectified auxiliary signal obtained from the EGM [13], [16], [18], [25], which estimates f_0 in the original EGM, as given by f_d in the auxiliary signal. This estimated f_0 was used for estimating the CL and to compute OA parameters. A spectral representation $P(f)$ was obtained for each EGM by using Welch periodogram with rectangular windowing, 2048 samples, 50% overlapping. These settings were used because previous experiments (not included here) showed that oi is reduced when time averaging is made using any windowing different from a rectangular structure. Hence, f_d was obtained as the maximum in the spectral representation of the EGM, and $P_n(f)$ as the unit-area normalized power spectrum at frequency f. Other conventional parameters were $bw(f_0)$, $bw(f_d)$, $P_n(f_0)$, $P_n(f_d)$, $P_n(f_k)$, oi, and ri.

The mean firing rates (MFRs) of the cell directly below the recording electrode were computed using the action potentials, for each simulated condition. For fibrillatory conduction, the MFR was also calculated using a square of nine cells directly below the recording electrode. MFR values can also be used as a gold standard for the main rhythm of the simulated EGM.

The averaged CL was also obtained in the time domain by an expert counting the EGM relevant peaks, aiming to establish their relationship with the spectral parameters, and also a means of evaluate the quality of the f_0 estimation.

C. Simulations Results

1) Results on Periodicity Parameters: Simulated EGM and their spectra are shown in Fig. 1, and Table I contains their measured spectral parameters for both DFA–OA and FOA procedures. A narrow-line spectral structure was observed in all cases, and a harmonic structure was present in all the recordings, except for fibrillatory conduction.

There was high agreement among f_0, as estimated by DFA and FOA, the inverse of CL, and the MFR, for the cases of plane wavefront, focal activation, and anchored rotor. The interharmonic separation between successive peaks in the spectra was also about f_0 Hz in these cases. Parameter f_d, when estimated directly from EGM spectrum, was the same as f_0 (both FOA and DFA estimated) only in the anchored rotor, but in plane wavefront and focal activation f_d corresponded to the second harmonic of f_0.

For fibrillatory conduction, a clear harmonic structure was not observed and a less narrow-band spectra was present. The inverse of the manually determined CL (6.9 Hz for monopolar and 8 Hz for bipolar) were more related to f_d (6.45 and 7.52 Hz) and f_0 estimated by FOA (7.49 and 7.53 Hz) than to f_0 estimated by DFA (4.6 and 3.1 Hz). The agreement between f_0 from FOA, in both monopolar and bipolar recordings, and MFR (7.08 Hz) is an additional indication of the robustness of the proposed method when estimating the main rhythm of EGM in complex conditions. The automatic algorithm for estimating f_0 using DFA was seen to fail here. Taking into account that it was still a narrow-band spectrum, it could be seen as a single-harmonic spectrum, and hence, the averaged CL would be consistently explained by f_d in this example. The values obtained for f_0 estimated by FOA were very similar for both monopolar and bipolar recordings.

2) Results on Spectral Envelope: The previously observed differences between f_0 and f_d were explained by the spectral envelopes of the EGM. As seen in Table I and Figs. 1 and 3, the harmonic peaks followed a smooth variation in the frequency domain, approximately corresponding to the spectral envelopes. In fibrillatory conduction, the spectral envelope was significantly different from the profile of the spectral peaks, given that the beat-to-beat variations were considerably higher. Nevertheless, the relative amplitude of the spectral lines was determined by the spectral envelope, and hence, this feature caused f_d to be

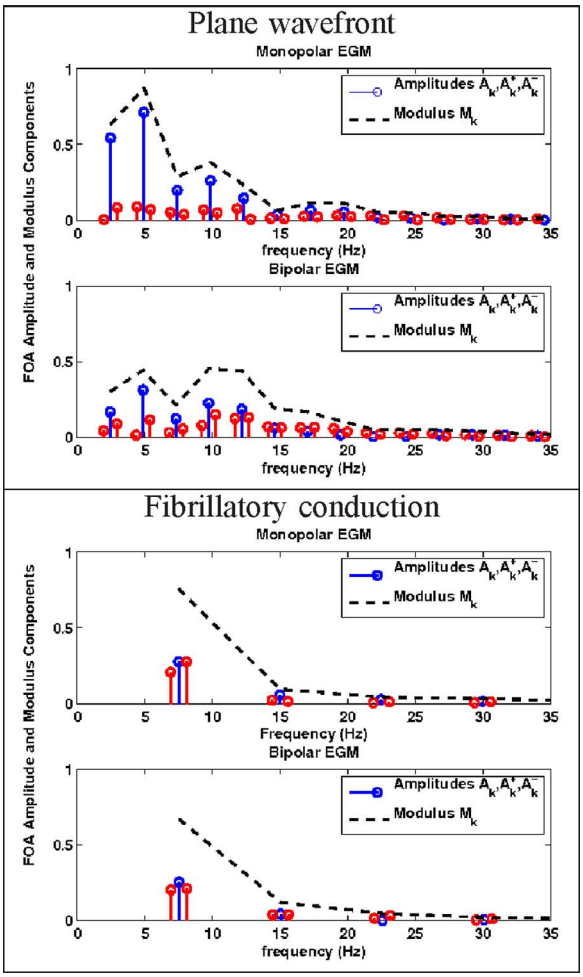

Fig. 3. Simulation results. Spectral envelope using amplitude and modulus components from FOA for (top) bipolar and (bottom) monopolar recordings in plane wavefront and fibrillatory conduction. Parameters M_k have been interpolated with splines for visualization and comparison purposes.

different from f_0. As shown in Table I, the harmonic peaks followed a profile similar to the FOA modulus.

Spectral envelope mainly depended on two causes, namely, the setting configuration of the acquisition lead system and the underlying electrophysiological process during each cycle. In our simulations, the same underlying electrophysiological process had a very different spectral shape, depending on the electrode configuration. As an example, the spectral envelope of bipolar EGM in the plane wavefront had a higher spectral content around 12 Hz when compared to the monopolar EGM. These differences between envelopes of different configurations were less evident in fibrillatory conduction, where the underlying electrophysiological activity was a faster, more high-frequency process, enough to partially compensate the effect of the lead configuration on the spectral envelope. Obviously, similar underlying electrophysiological activations will exhibit similar spectral envelopes under the same lead configuration (e.g., plane wavefront versus focal activation examples), but different envelopes with different electrophysiological activations (e.g., plane wavefront versus fibrillatory activity examples).

3) Results on Organization Parameters: Table I also shows the parameters related to OA (oi and ri), and parameters p_1 and p_e from FOA. Bandwidth tended to be higher in bipolar than in monopolar EGM. For regular rhythms, organization, as quantified with oi and p_1, was high both for monopolar and for bipolar recordings, with a trend in monopolar EGM to be higher than in bipolar EGM. However, organization was much lower in these recordings, as quantified by ri, since this parameter does not consider the organized activity contained in the harmonics. Irregular rhythms exhibited dramatically lower oi and p_1, as expected in fibrillatory conduction. However, since oi is computed from the estimation of f_0, it is necessary to be sure that f_0 is correctly estimated, otherwise the interpretation of oi values could be misleading. The high irregularity of the fibrillatory conduction can be observed from the FOA amplitude components $\{A_1^-, A_1^+\}$ in Fig. 3, being very similar to the FOA amplitude component A_1. However, these components were considerably lower than component A_1 for more regular rhythms.

V. Results on Clinical Databases

A. Databases

Two different databases with EGM recordings stored in ICD were used in this study. All the EGM recordings were obtained from patients undergoing the implant of a Medtronic device in Hospital Universitario Virgen de la Arrixaca of Murcia and in Hospital General Universitario Gregorio Marañón of Madrid, Spain. For each analyzed episode, two simultaneously recorded EGM were available in the device, with pseudomonopolar (from can to coil) and bipolar (from tip to ring) configurations, at 128 samples per second. Recordings included in the study were revised and classified by an specialist.

There is little information in the literature about regularity measurements for other rhythms than VF, as given by the ECG or the EGM waveforms. However, it is widely known that the SR has a fluctuating magnitude due to heart rate variability, and also, VT are known to be less stable in instantaneous rhythm than SVT. Hence, we wanted to test whether the known differences among rhythms, in terms of instantaneous cycle, were coherent with the organization parameters on the EGM waveforms.

The first clinical database consisted of EGM during four different rhythms, namely, five SR, eight SupraVT (SVT), eight VT, and seven VF. AF recordings were discarded for this study, whereas SVT and VT were collected by requiring relatively stable episodes along the whole recording. Additionally, SVT were considered in which a similar morphology to SR could be observed, and VT were recognized by an expert in those episodes with very different morphology from SR. We only considered one episode per patient, and small yet balanced groups were assembled. The analysis in this database aimed to assess the performance of FOA procedure in sustained and nonsustained rhythms, with some similarity to the simulation conditions in the preceding sections. All EGM recordings in this database had the same length (6 s), except for one of the five SR signals, which had 4.8 s length. The second clinical database consisted of EGM only from VF, specifically, up to 240 VF episodes in 99 patients, for which we used all the available time recorded for

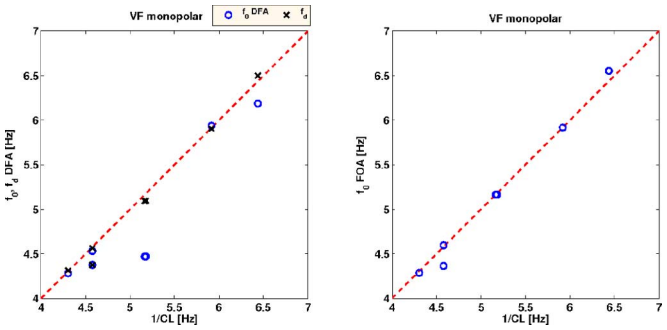

Fig. 4. Relationship between f_d and f_0 from DFA and FOA, and $1/\mathrm{CL}$ for every single one VF EGM in first database with different rhythms.

each EGM signal. In this set of recordings, we aimed to check whether failures of the automated algorithm used for estimating f_0 in DFA and OA could have an impact on a larger set of measurements, and to check whether FOA could give high-quality measurements in the same conditions.

Each EGM in both clinical databases was analyzed, following the same methodology used in the previous section, both for conventional analysis given by DFA and OA and for the proposed FOA method. The averaged $1/\mathrm{CL}$ in the time domain was also obtained for each EGM given by manual annotation by an expert, which allowed us to establish a gold standard for comparison with periodicity estimations from the classical and the proposed method.

B. Results on Database With Different Rhythms

Table II contains the averaged $1/\mathrm{CL}$ from manual annotation for each EGM in the database with different rhythms, and the measured spectral parameters when computed with both DFA and FOA approaches (mean $\pm$ standard deviation for all of them). There was a high agreement between $1/\mathrm{CL}$ and f_0 computed using FOA method for all rhythms, both in monopolar and bipolar recordings, indicating that FOA method is more suitable in the estimation of the main rhythm, whereas f_0 computed using DFA and f_d showed only good agreement in VF recordings. Moreover, as shown in Fig. 4, the proposed FOA was more accurate than DFA when estimating the averaged $1/\mathrm{CL}$ for every single VF episode.

There was also visible discrepancy between f_0 when computed using DFA and FOA in SR recordings. Given that DFA gave higher values of f_0 both in monopolar and bipolar recordings than FOA, and the DFA method tended, in general, to overestimate f_0 when compared to FOA. Another suggestion that FOA gave better estimates was the agreement between f_0 when computed in monopolar and in bipolar recordings. Also, f_0 computed by FOA allowed coherent comparisons between different rhythms. The slowest CL was for SR and the fastest was for VF, as trivially expected, whereas SVT and VT were very similar in terms of CL. Fig. 5 shows the spline-interpolated, normalized, and averaged spectral envelopes for the four rhythms. Bipolar recordings generally contained more power in high-frequency components than monopolar recordings, and there was a crossing point in the spectral envelopes in SR, SVT, and VT, but

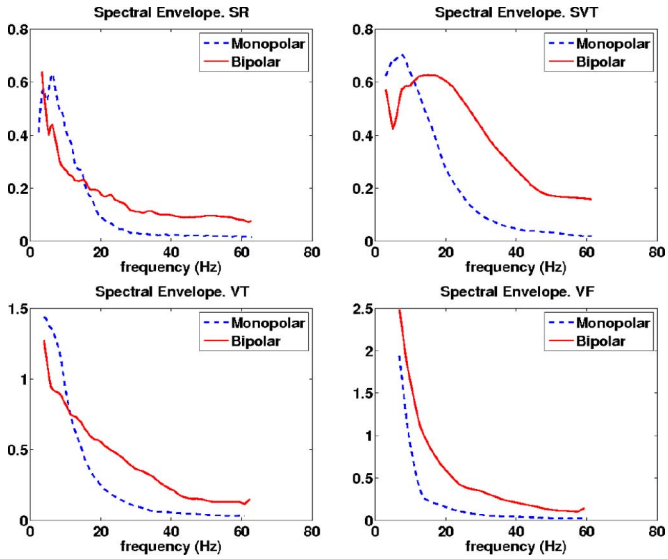

Fig. 5. Averaged spectral envelopes (using spline-interpolated amplitudes) of the FOA signal model for the database with different rhythms.

not in VF. Table II also shows parameters oi and ri from OA and parameters p_1 and p_e from FOA. Interpretation of the EGM organization has to be done with caution when using OA parameters, since they are based on f_0 estimation and, as previously stated, the automatic estimation procedure in conventional DFA failed in several cases. According to oi, SR was more irregular than SVT, than VT, and also than VF when obtained from OA. FOA approach made it possible to establish a more coherent organization comparisons. According to p_1 in FOA, VF was the most irregular rhythm, as expected, whereas SVT was the most organized, even more than SR, which can be explained by the well-known heart rate variability due to the autonomous system control of cardiac cycle in healthy conditions.

C. Results on Database With VF

Table III shows the spectral parameters measured by DFA and by FOA in the database with VF episodes. Periodicity, as characterized by f_0, was slightly different when estimated by DFA and by FOA. Further details can be seen in Fig. 6, which shows f_0 as estimated by DFA versus f_0 as estimated by FOA, thus allowing us to compare both estimations without the averaging effect in Table III. Note that though, in general terms, there was a high agreement between both estimations; however, in some cases, the estimation of f_0 was dramatically different. Moreover, there was higher agreement between f_d and f_0 estimated by FOA than between f_d and f_0 estimated by DFA. This result is consistent with previous results in simulated signals and first database of real signals, showing that for nonharmonic structure, e.g. VF recordings, f_0 estimated by FOA is related to f_d. The differences between f_0 estimated by DFA and by FOA and between f_d and f_0 by DFA were significant (paired t-test, $p < 0.05$); whereas the differences in f_0 by FOA and f_d were nonsignificant, both in monopolar and bipolar recordings. Therefore, we can conclude that FOA yields better estimations

TABLE II
RESULTS OF DFA, OA, AND FOA IN CLINICAL EGM SIGNALS FROM THE DIFFERENT RHYTHMS DATABASE.

		Sinus Rhythm		Supraventricular Tachycardia		Ventricular Tachycardia		Ventricular Fibrillation	
		Monopolar	Bipolar	Monopolar	Bipolar	Monopolar	Bipolar	Monopolar	Bipolar
Time	CL^{-1} (Hz)	1.21 ± 0.11	1.21 ± 0.11	2.58 ± 0.15	2.58 ± 0.16	2.72 ± 0.47	2.71 ± 0.47	5.16 ± 0.78	5.20 ± 0.84
DFA and OA	f_0 (Hz)	2.94 ± 0.76	3.66 ± 0.33	2.58 ± 0.16	3.51 ± 1.2	3.25 ± 0.67	3.25 ± 0.66	5.10 ± 0.87	5.25 ± 0.82
	f_d (Hz)	3.94 ± 0.90	4.03 ± 2.67	6.62 ± 3.78	9.36 ± 11.68	5.36 ± 2.58	5.34 ± 4.62	5.24 ± 0.87	5.26 ± 0.85
	ri	0.15 ± 0.01	0.21 ± 0.25	0.26 ± 0.11	0.15 ± 0.04	0.35 ± 0.19	0.51 ± 0.70	0.71 ± 0.09	0.49 ± 0.11
	oi	0.47 ± 0.04	0.48 ± 0.19	0.92 ± 0.02	0.64 ± 0.02	0.84 ± 0.21	0.81 ± 0.28	0.81 ± 0.06	0.74 ± 0.08
FOA	f_0 (Hz)	1.22 ± 0.11	1.22 ± 0.11	2.58 ± 0.16	2.58 ± 0.16	2.74 ± 0.46	2.70 ± 0.52	5.26 ± 0.89	5.27 ± 0.87
	p_1	0.82 ± 0.12	0.68 ± 0.13	0.91 ± 0.08	0.70 ± 0.23	0.74 ± 0.21	0.64 ± 0.27	0.66 ± 0.15	0.51 ± 0.09
	p_e	0.18 ± 0.12	0.32 ± 0.13	0.09 ± 0.08	0.30 ± 0.23	0.26 ± 0.21	0.36 ± 0.27	0.34 ± 0.15	0.49 ± 0.09

TABLE III
RESULTS OF DFA, OA, AND FOA IN CLINICAL EGM SIGNALS FROM VF DATABASE

	DFA		FOA	
	Monopolar	Bipolar	Monopolar	Bipolar
f_0 (Hz)	4.68 ± 0.73	4.67 ± 0.84	4.85 ± 0.82	4.85 ± 1.00
p_1	—	—	0.50 ± 0.20	0.37 ± 0.20
p_e	—	—	0.50 ± 0.21	0.63 ± 0.20
f_d (Hz)	4.90 ± 1.07	4.90 ± 1.71	—	—
ri (OA)	0.56 ± 0.18	0.37 ± 0.18	—	—
oi (OA)	0.73 ± 0.16	0.62 ± 0.15	—	—

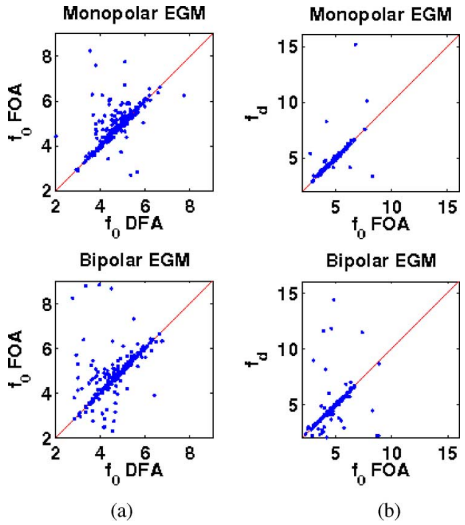

Fig. 6. Estimation of f_0 by (a) DFA and (b) f_d versus f_0 estimated by FOA for each EGM recording in VF database. The red line represents the $y = x$ line; points in this line representing both methods yielding the same estimated frequency.

of f_0 than the automatic procedure in DFA for VF recordings stored in ICD.

Organization parameters, namely oi and ri in OA, and p_1 and p_e in FOA, showed again and consistently that bipolar recordings are in general less organized than monopolar recordings.

VI. DISCUSSION AND CONCLUSION

A new algorithm has been presented as a generalization of conventional DFA and OA, so-called FOA, which allows us to automatically obtain the spectral structure and features in EGM recordings. Controlled electrophysiological substrates have been simulated, and synthetic EGM have been obtained. A small database with four different rhythms and an extensive VF database have also been analyzed. The database with different rhythms aimed to evaluate the performance of the two different approaches, the classical DFA and the proposed FOA, in real EGM recordings with different electrophysiological and well-known situations. On the other hand, VF database aimed to evaluate the performance of both approaches in a real database with a large number of EGM recording. This was necessary to determine that the failures associated with the algorithm used in conventional DFA for estimating f_0 had some visible impact on the estimated regularity in a populational analysis. It also showed that the use of FOA alleviated the impact of these failures. This methodology allowed us to give a principled understanding of the meaning and limitations of the different indexes currently used in the DFA and OA literature, and also to check the improvement given by the FOA spectral description.

A. Fundamental and Dominant Frequency

Due to a number of factors, f_0 and f_d can be different, and in that case, the use of f_d as a surrogate for the CL is not guaranteed. This is because it might be just a harmonic of f_0. It is clearly shown in our results, suggesting that a distinction between f_d and f_0 should be maintained, in order to avoid errors in the determination of the EGM-approximate CL. The virtually universal use of f_d in the electrophysiology literature should not lead to the erroneous concept that f_d always corresponds to the CL of the EGM. When harmonic structure is present, the interharmonic separation can confirm the estimated CL.

A usual procedure in DFA consists of estimating f_d from an auxiliary signal obtained by filtering and rectification of the original EGM [13], [16], [18], [25]. In these references, this auxiliary signal was used to calculate f_0 in the bipolar EGM, either for calculating the CL or as complementary information for the calculation of the oi. If the calculations have been successful, f_d in the auxiliary signal will correspond to f_0 in the original EGM. However, this will not be always the case, and sometimes an error in this automatic algorithm will yield incorrect CL estimations. In [25], an example is presented [25, Fig. 5(b)] of an irregular EGM in which DFA gives a 10-Hz peak. In this case, the comparison to the activation interval pointed out by the authors, together with the evident presence of harmonic structure, indicates that the periodicity was given by f_0 at the 5 Hz peak, and that f_d was just its second harmonic. In a study examining the effect of changes in atrial EGM during AF on the f_d [28], good agreement was, in general, obtained between the (inverse of the) averaged CL and the f_d, except for varying amplitude and activation interval conditions [28, Fig. 3(d)]. Problems in the estimation of the CL therein can be explained by the automatic

algorithm failing to extract the peak from the auxiliary signal, and they are similar to the ones observed in our experiments with VF recordings (see Section V).

The procedure that we presented here to estimate f_0 using FOA gave better results than the classical DFA procedure due to the fact that FOA is implicitly based on the harmonic structure presented in the signal to model it. FOA also accounts for fluctuations in the harmonic components, and the interharmonic spacing of the spectral peaks can give relevant information about the averaged CL of an EGM. The estimated CL in the spectral domain could also be cross-checked with the time domain estimated in case of doubts. However, cross-checking with time-peaks counting can introduce some subjectivity or doubts, whereas MSE minimization is an objective and quantitative criterion. In fibrillatory recordings, FOA also performs well, because the LS projection gives a relevant weight only to the f_0 component, which in this case corresponds to f_d.

It should be noted that when a nonharmonic spectral structure is present, the f_0 parameter estimated with FOA can be similar to the f_d parameter, which will be a common situation in VF. Still, aiming to give an automated procedure, we decided to always look for f_0 parameter in the EGM to capture the periodicity of the main rhythm. Taking into account the results of Table II (VF column), even in those cases of VF with one main narrow component and widespread activity, f_0 is often coincident with f_d, and both parameters keep a marked coherence with $1/\mathrm{CL}$, as marked by an expert. Hence, for the algorithm giving a unified solution, we can consider that in those cases with one single narrow main component, we have a harmonic structure with one single harmonic. This unification in the result of the algorithm for periodicity estimation has to be clearly complemented with a parameter for regularity characterization.

B. Acquisition in Bipolar and Monopolar Recordings

Because the spectral envelope is simultaneously determined by the underlying physiological process and by the characteristics of the acquisition system, its quantification, either in terms of the power of the harmonics or by a more detailed and sophisticated technique, can yield a more detailed spectral description of the EGM under study. In general, f_d and f_0 are more likely to be coincident in monopolar than in bipolar recordings. The monopolar EGM can be said to have a mostly low-pass (bandpass) spectral envelope. Optical mapping recordings during AF and VF usually have a low-pass spectral envelope [17], [29], and hence, f_0 and f_d were usually the same in these recordings, which avoided the need of using the auxiliary signal processing. However, monopolar and bipolar atrial EGM during AF will have low-pass and band-pass envelopes, respectively, and comparisons between spectral parameters obtained from different systems can be problematic, given that small differences in the acquisition system (such as, interelectrode spacing or electrode size) could produce significant differences in the spectral envelope.

C. Organization and Harmonics

In the presence of harmonic structure, an appropriate signal model of organization should take the harmonics into consideration. Given that ri parameter was initially defined for optical mapping recordings, it could have some interpretation problems when straightforwardly applied to EGM during AF. This is due to the presence of harmonics. In this case, a redefinition of organization according to the spectral characteristics of the analyzed EGM is convenient. This is done in [13], where Everett *et al.* defined oi. A theoretical study on OA for bipolar EGM [30] showed that the calculation of ri could be affected by harmonics, and concluded that the ri is not a valid measure for organization. The conclusion might have changed if the harmonic structure of the bipolar EGM had been considered. FOA in our simulation and real data studies shows that regularity measurements have to account for the harmonics in its definition. Otherwise, misleading low values of organization can be obtained from organized EGM recordings. The use of oi is more robust in this sense than ri, but still it can be affected by poor previous estimation of the periodicity parameter.

D. Additional Considerations

One possible improvement for the method proposed is to look for Δ in a narrow frequency interval around the harmonic peaks, in order to capture more wideband behaviors. However, the usefulness of this modification was not significant in our database (not shown). We also analyzed the arrhythmia discrimination capabilities of the parameters, keeping in mind the limited size of the first dataset. In this setting, parameters from the FOA approach, f_0 and p_1, were the only ones that seemed to offer a coherent trend for rhythm classification. We further analyzed the effect of the recording length in the second database, and found that the averaged differences between a fixed length for all the recordings (6 s) and the actual length of the episode being considered were not relevant. However, in few cases, some problems could arise when using a different frequency grid for the same EGM, which is an effect to be taken into account in the algorithm.

E. Limitations of the Study

The mathematical model that has been used in the present study is approximated and highly simplified. The simulation of complex electrophysiological conditions could lead to inaccurate morphology for the extracellular signals, since in complex conditions, the amplitude and morphology of the action potentials may be highly variable. The use of computer models based on differential equations would be more appropriate when simulating and analyzing a wider variety of VF mechanisms. Accordingly, extrapolation of the results to the clinical environment should be made cautiously. Results on ICD recordings were significant, but their extrapolation to electrical and optical mapping recordings should be specifically addressed. While we focused on VF recordings, FOA algorithm can be used for analyzing AF EGM, which is an interesting research direction. Also of interest is the consideration of several periodic components in the signal under analysis. These two relevant issues are beyond the scope of this paper.

F. Conclusion

DFA and OA of EGM have been used in cardiac electrophysiology for characterizing almost-periodic activation and high regularity regions, respectively. The rationale under the mathematical definition of these indexes has not always been fully considered, thus leading to interpretation problems. Our results show that the proposed FOA yields a more compact and reliable organization description of cardiac EGM than DFA and OA alone in ICD-stored EGM signals.

ACKNOWLEDGMENT

The authors would like to thank Dr. M. R. Wilby for proofreading and English review, and to the anonymous reviewers for their useful comments and suggestions.

REFERENCES

[1] M. Biermann, M. Shenasa, M. Borggrefe, G. Hindricks, W. Haverkamp, and G. Breithardt, "The interpretation of cardiac electrograms," in *Cardiac Mapping*. Mount Kisco, NY: Futura, 1993.

[2] W. M. Smith, J. M. Wharton, and S. M. Blanchard, "Direct cardiac mapping," in *Cardiac Electrophysiology: From Cell to Bedside*. Philadelphia, PA: Saunders, 1990.

[3] T. Taneja, J. Goldberger, M. A. Parker, D. Johnson, N. Robinson, G. Horvath, and A. H. Kadish, "Reproducibility of ventricular fibrillation characteristics in patients undergoing implantable cardioverter defibillator implantation," *J. Cardiovasc. Electrophysiol.*, vol. 8, pp. 1209–1217, 1997.

[4] L. Morkrid, O. J. Ohm, and H. Engedal, "Time domain and spectral analysis of electrograms in man during regular ventricular activity and ventricular fibrillation," *IEEE Trans. Biomed. Eng.*, vol. BME-31, no. 4, pp. 350–355, Apr. 1984.

[5] P. Sanders, O. Berenfeld, M. Hocini, P. Jaïs, R. Vaidyanathan, L. F. Hsu, S. Garrigue, Y. Takahashi, M. Rotter, F. Sacher, C. Scavée, R. Ploutz-Snyder, J. Jalife, and M. Haïsaguerre, "Spectral analysis identifies sites of high-frequency activity maintaining atrial fibrillation in humans," *Circulation*, vol. 112, pp. 789–797, 2005.

[6] F. Atienza, J. Almendral, J. Moreno, R. Vaidyanathan, A. Talkachou, J. Kalifa, A. Arenal, J. P. Villacastín, E. G. Torrecilla, A. Sánchez, R. Ploutz-Snyder, J. Jalife, and O. Berenfeld, "Activation of inward rectifier potassium channels accelerates atrial fibrillation in humans: Evidence for a reentran mechanism," *Circulation*, vol. 114, pp. 2434–2442, 2006.

[7] A. C. Skanes, R. Mandapati, O. Berenfeld, J. M. Davidenko, and J. Jalife, "Spatiotemporal periodicity during atrial fibrillation in the isolated sheep heart," *Circulation*, vol. 98, pp. 1236–1248, 1998.

[8] H. S. Karagueuzian, S. S. Khan, W. Peters, W. J. Mandel, and G. A. Diamond, "Nonhomogeneous local atrial activity during acute atrial fibrillation: Spectral and dynamic analysis," *PACE*, vol. 13, pp. 1937–1942, 1990.

[9] D. S. Rosenbaum and R. J. Cohen, "Frequency based measures of atrial fibrillation in man," in *Proc. IEEE Eng. Med. Biol. Soc.*, 1990, vol. 12, pp. 582–583.

[10] J. Chen, R. Mandapati, O. Berenfeld, A. C. Skanes, and J. Jalife, "High-frequency periodic sources underlie ventricular fibrillation in the isolated rabbit heart," *Circ. Res.*, vol. 86, pp. 86–93, 2000.

[11] A. V. Zaitsev, O. Berenfeld, S. F. Mironov, J. Jalife, and A. M. Pertsov, "Distribution of excitation frequencies on the epicardial and endocardial surfaces of fibrillating ventricular wall of the sheep heart," *Circ. Res.*, vol. 86, pp. 408–417, 2000.

[12] A. Casaleggio, P. Rossi, A. Faini, T. Guidotto, V. Malavasi, G. Musso, and G. Sartori, "Analysis of implantable cardioverter defibrillator signals for non conventional cardiac electrical activity characterization," *Med. Biol. Eng. Comput.*, vol. 44, pp. 45–53, 2006.

[13] T. H. Everett, J. R. Moorman, L. C. Kok, J. G. Akar, and D. E. Haines, "Assessment of global atrial fibrillation organization to optimize timing of atrial defibrillation," *Circulation*, vol. 103, pp. 2857–2861, 2001.

[14] S. Singh, E. Heist, J. Koruth, C. Barrett, J. Ruskin, and M. Mansour, "The relationship between electrogram cycle length and dominant frequency in patients with persistent atrial fibrillation," *J. Cardiovasc. Electrophysiol.*, vol. 20, no. 12, pp. 1336–1342, 2009.

[15] O. Barquero-Pérez, J. L. Rojo-Álvarez, J. Requena-Carrión, F. Alonso Atienza, E. Everss, R. Goya Esteban, J. J. Sánchez-Muñoz, and A. GarcíaAlberola, "Cardiac arrhythmia spectral analysis of electrogram signals using fourier organization analysis," presented at the Comput. Cardiol., Park City, Utah, 2009.

[16] J. Ng, A. Kadish, and J. J. Goldberger, "Technical considerations for dominant frequency analysis," *J. Cardiovasc. Electrophysiol.*, vol. 18, pp. 757–764, 2007.

[17] F. H. Samie, O. Berenfeld, J. Anumonwo, S. F. Mironov, S. Uassi, J. Beaumont, S. Taffet, A. M. Pertsov, and J. Jalife, "Rectification of the background potassium current: A determinant of rotor dynamics in ventricular fibrillation," *Circ. Res.*, vol. 89, pp. 1216–1223, 2001.

[18] T. H. Everett, L. C. Kok, J. R. Moorman, and D. E. Haines, "Frequency domain algorithm for quantifying atrial fibrillation organization to increase defibrillation efficacy," *IEEE Trans. Biomed. Eng.*, vol. 48, no. 9, pp. 969–978, Sep. 2001.

[19] J. J. Sánchez-Muñoz, J. L. Rojo-Álvarez, A. García-Alberola, E. Everss, F. Alonso-Atienza, M. Ortiz, J. Martínez-Sánchez, J. Ramos-López, and M. Valdés, "Spectral analysis of intracardiac electrograms during induced and spontaneous ventricular fibrillation in humans," *Europace*, vol. 11, pp. 328–331, 2009.

[20] J. J. Sánchez-Muñoz, J. L. Rojo-Álvarez, A. García-Alberola, J. Requena-Carrión, E. Everss, M. Ortiz, J. Martínez-Sánchez, and M. Valdés, "Spectral analysis of sustained and non-sustained ventricular fibrillation in patients with an implantable cardioverter-defibrillator," *Revista Española de Cardiología*, vol. 62, pp. 690–693, 2009.

[21] J. J. Sánchez-Muñoz, J. L. Rojo-Álvarez, A. García-Alberola, E. Everss, J. Requena-Carrión, M. Ortiz, F. Alonso-Atienza, and M. Valdés, "Effects of the location of myocardial infarction on the spectral characteristics of ventricular fibrillation," *PACE*, vol. 31, pp. 660–665, 2008.

[22] J. L. Rojo-Álvarez, A. Arenal-Maíz, and A. Artés-Rodríguez, "Support vector black-box interpretation in ventricular arrhythmia discrimination," *IEEE Eng. Med. Biol.*, vol. 21, no. 1, pp. 27–35, Jan./Feb. 2002.

[23] K. Minami, H. Nakajima, and T. Toyoshima, "Real-time discrimination of ventricular tachyarrhythmia with Fourier-transform neural network," *IEEE Trans. Biomed. Eng.*, vol. 46, no. 2, pp. 179–185, Feb. 1999.

[24] J. W. Picone, "Signal modelling techniques in speech recognition," *Proc. IEEE*, vol. 81, no. 9, pp. 1215–1247, Sep. 1993.

[25] J. Ng and J. J. Goldberger, "Understanding and interpreting dominant frequency analysis of AF electrograms," *J. Cardiovasc. Electrophysiol.*, vol. 18, pp. 680–685, 2007.

[26] F. Alonso-Atienza, J. Requena-Carrión, A. García-Alberola, J. L. Rojo-Álvarez, J. J. Sánchez-Muñoz, J. Martínez-Sánchez, and M. Valdés, "A probabilistic model of cardiac electrical activity based on a cellular automata system," *Revista Española de Cardiología*, vol. 58, pp. 41–47, 2005.

[27] J. Malmivuo and R. Plonsey, *Principles and Applications of Bioelectric and Biomagnetic Fields*. New York: Oxford Univ. Press, 1995.

[28] J. Ng, A. H. Kadish, and J. J. Goldberger, "Effect of electrogram characteristics on the relationship of dominant frequency to atrial activation rate in atrial fibrillation," *Heart Rhythm*, vol. 3, pp. 1295–1305, 2006.

[29] J. Kalifa, K. Tanaka, A. V. Zaitsev, M. Warren, R. Vaidyanathan, D. Auerbach, S. Pandit, K. L. Vikstrom, R. Ploutz-Snyder, A. Talkachou, F. Atienza, G. Guiraudon, J. Jalife, and O. Berenfeld, "Mechanisms of wave fractionation at boundaries of high-frequency excitation in the posterior left atrium of the isolated sheep heart during atrial fibrillation," *Circulation*, vol. 113, pp. 626–633, 2006.

[30] G. Fischer, M. C. Stuhlinger, C. N. Nowak, L. Wieser, B. Tilg, and F. Hintringer, "On computing dominant frequency from bipolar intracardiac electrograms," *IEEE Trans. Biomed. Eng.*, vol. 54, no. 1, pp. 165–169, Jan. 2007.

Author's photographs and biographies not available at the time of publication.